

Contents lists available at [ScienceDirect](https://www.sciencedirect.com)

## Expert Systems With Applications

journal homepage: [www.elsevier.com/locate/eswa](http://www.elsevier.com/locate/eswa)

# Adjusted Iterated Greedy for the optimization of additive manufacturing scheduling problems

Kuo-Ching Ying<sup>a,1</sup>, Fabio Fruggiero<sup>b,2</sup>, Pourya Pourhejazy<sup>c,\*,3</sup>, Bo-Yun Lee<sup>a,d,4</sup>

<sup>a</sup> Department of Industrial Engineering and Management, National Taipei University of Technology, Taipei 10608, Taiwan

<sup>b</sup> School of Engineering, University of Basilicata, Potenza 85100, Italy

<sup>c</sup> Department of Industrial Engineering, UiT- The Arctic University of Norway, Lodve Langsgate 2, Narvik 8514, Norway

<sup>d</sup> United Microelectronics Corporation, Hsinchu Science Park, Hsinchu 30073, Taiwan

## ARTICLE INFO

## Keywords:

Operations management  
Additive manufacturing  
3D printing  
Extrusion-based production scheduling  
Optimization

## ABSTRACT

As a disruptive technology, additive manufacturing (AM) is revolutionizing manufacturing supply chains. AM consists of producing 3-dimensional objects through layer-by-layer addition of compound material based on digital models. The scheduling of additive manufacturing operations differs from traditional (i.e., subtractive and injection molding) manufacturing with a single production run involving several parts/geometries;; this makes the jobs heterogeneous. Limited studies have investigated the Additive Manufacturing Scheduling Problems (AMSP). This study extends the Iterated Greedy algorithm to solve the AMSPs considering a single-machine production setting. For this purpose, several computational mechanisms are customized to account for AM-specific characteristics of production scheduling. Numerical analysis shows that the vast majority of the best-found solutions are yielded by the Adjusted Iterated Greedy (AIG) algorithm considering both solution quality and stability; the outperformance becomes more significant with an increase in problem size. Statistical analysis confirms that AIG's performance is notably better than that of the existing solution algorithm in terms of solution quality and stability. This study is concluded by providing directions for future development of AM and AMSPs to extend the industrial reach of 3D printing technology.

## 1. Introduction

Supply chain and product impacts of additive manufacturing, and its advantages over the traditional manufacturing techniques have made 3D printing a fast-growing new technology (Haghdadi et al., 2021). Recent advances, notably in the accuracy, time, and cost-efficiency of 3D printing, extend its application areas beyond rapid prototyping to end-part manufacturing (Salmi et al., 2016), which is paving the way for mass customization. In addition to the production sector, additive manufacturing has found its way in other industries, like construction (Paolini et al., 2019), energy (Sun et al., 2021), aerospace (Blakey-Milner et al., 2021), aviation (Gisario et al., 2019), pharmaceutical (Durga Prasad Reddy & Sharma, 2020), and disaster response (Tönissen & Schlicher, 2021). Additive manufacturing has implications

for industry 4.0 (Sepasgozar et al., 2020), circular economy (Cruz Sanchez et al., 2020), and social sustainability (Naghshineh et al., 2021). As a disruptive new technology, however, additive manufacturing requires substantially more development in the operations management literature for wider industrial reach.

Regardless of the technology type, additive manufacturing is different from subtractive manufacturing, like traditional milling, in that the traditional approach carves and cuts the raw material and requires additional procedures like forging, grinding, drilling, and assembly to complete the production of the final product. In contrast, 3D printing uses digital model data to make 3-dimensional objects through layer-by-layer addition of compound material (Vernon & Peckham, 2002). In this definition, several machines are required to complete the production process in subtractive manufacturing, depending on the design complexity, while 3D printers can handle high complexity

\* Corresponding author.

E-mail addresses: [kcying@ntut.edu.tw](mailto:kcying@ntut.edu.tw) (K.-C. Ying), [fabio.fruggiero@unibas.it](mailto:fabio.fruggiero@unibas.it) (F. Fruggiero), [pourya.pourhejazy@uit.no](mailto:pourya.pourhejazy@uit.no) (P. Pourhejazy).

<sup>1</sup> 0000-0002-9549-5290.

<sup>2</sup> 0000-0001-9412-6605.

<sup>3</sup> 0000-0002-1207-3587.

<sup>4</sup> 0000-0001-9611-2557.

<https://doi.org/10.1016/j.eswa.2022.116908>

Received 3 November 2021; Received in revised form 26 January 2022; Accepted 12 March 2022

Available online 19 March 2022

0957-4174/© 2022 The Author(s). Published by Elsevier Ltd. This is an open access article under the CC BY license (<http://creativecommons.org/licenses/by/4.0/>).

**Notations**

$i$	Geometry tag, $i \in \{1, 2, \dots, n_g\}$
$j$	Build tag, $j \in \{1, 2, \dots, n_b\}$
$n_g$	Total number of orders (geometries)
$n_b$	Number of the builds.
$\alpha, \beta, \gamma$	Earliness, tardiness, and cost constant weights
$E_i$	Earliness of geometry $i$
$T_i$	Tardiness of geometry $i$
$V_{chamber}$	Build chamber volume
$V_i$	Volume of geometry $i$
$d_i$	Demand of geometry $i$
$TOC_i$	Total order cost of geometry $i$ .
$n_{i,j}$	Number of $i$ th geometry in build $j$ .

products more efficiently, enabling easier assembly and toughness (Pérez et al., 2020; Song et al., 2017).

Given the differences between additive and traditional manufacturing, optimization and decision analysis subjects, like preventive maintenance, process design, capacity planning, resource planning, inventory management, human factors, facility planning, and production scheduling and planning require investigation (Khorram Niaki & Nonino, 2017). From the early studies, Ransikarbum et al. (Ransikarbum et al., 2017) developed a decision-aid method for multi-objective optimization of a batch of parts and multiple printers, and (Rudolph & Emmelmann, 2017) introduced a cloud-based platform for the order management of additive manufacturing-based production systems. There are many other studies on managerial theories and approaches considering the emergence of additive manufacturing (see (Khorram Niaki & Nonino, 2017; Sonar et al., 2020)). Low productivity and operational uncertainties are the main barriers to extending additive manufacturing applications to final-part manufacturing and mass customization (Bikas et al., 2016). Despite the relevance of planning and scheduling of additive manufacturing operations in addressing these barriers, the research on this topic remains limited.

From a production scheduling standpoint, the additive and subtractive production scheduling vary in that a particular production run may have to deal with several geometries, each of which constitutes generic jobs. The study of (Li et al., 2017) was the first to investigate machine scheduling problems under this definition. Later, (L. Zhou et al., 2018) explored a multi-task scheduling problem for distributed manufacturing using 3D printing services. Considering the type of printing operation, the existing problems can be categorized into three groups. The first group, Nesting for Additive Manufacturing (NfAM), investigates the problem of arranging parts into the printer (build) to maximize the number of prints and the utilization of chamber volume without providing the production schedule (Zhang et al., 2018). The second group, i.e., Scheduling for Additive Manufacturing (SfAM), explores the positioning of the builds' print sequence to enhance productivity; the recent studies by (Luzon & Khmel'nitsky, 2019; Oh et al., 2018) are prime examples of this type of approach for scheduling printing operations in additive manufacturing. These studies do not account for the nesting process of the builds; nesting is different from grouping in that builds can be generated by a bin-packing algorithm to assign parts into multiple builds (Nesting) while parts can be clustered into builds considering the builds' physical constraints (Grouping). The third group is a combination of NfAM and SfAM, hereafter referred to as Nesting and Scheduling for Additive Manufacturing (NSfAM), which simultaneously considers the nesting and process scheduling decisions. (Oh et al., 2020) suggested to integrate the nesting and scheduling problems because they are interrelated. They classified the NSfAM considering the number of parts, builds, and machines. In additive manufacturing, parts usually cannot be printed entirely using one build, i.e., due to physical

limitations; hence, multiple builds are required to complete the 3D printing procedure. On this basis, the problem of multi-parts, multi-builds, and a single 3D printing machine, which is denoted by (M/M/S) and is of practical interest, is the focus of the present article.

To the best of the authors' knowledge, the literature of Additive Manufacturing Scheduling Problem (AMSP) under (M/M/S) setting is limited to a few papers. In an early study, (Kucukkoc, 2019) addressed the AMSPs on a single machine developing a mixed-integer linear programming formulation. The basic AMSP formulation was later extended by (Arik, 2021) to account for the assembly operation of the parts after processing them on a 3D printer. These two studies used exact solution methods for solving very small instances. (Fera et al., 2018) developed an improved Genetic Algorithm to solve larger instances, showing that the algorithm performs well in a single machine production setting. Most recently, (Fera et al., 2020) developed an Improved Tabu Search (ITS) algorithm to solve the same problem; they showed that their algorithm outperforms the earlier metaheuristic in solving small- to large-scale instances. Inspired by the limited research on AMSPs, the present study develops a competitive benchmark algorithm to improve the Best-Found Solutions (BFS) to the existing test instances by (Fera et al., 2020). For this purpose, the Adjusted Iterated Greedy (AIG) is developed that entails customized operators for the effective approximation of the AMSPs. The test instances are also extended to form a testbed for a more comprehensive benchmark in additive manufacturing.

The remainder of this manuscript begins with an introduction of AMSPs in Section 2. The proposed algorithm is then presented in Section 3. Experimental results and statistical analysis are provided in Section 4 to evaluate the performance of the developed algorithm benchmarking it against the current-best-performing algorithm in the literature of AMSPs. Finally, the concluding remarks and suggestions for future research directions are provided in Section 5.

## 2. Additive manufacturing scheduling problems

Additive manufacturing, also known as rapid prototyping, layer manufacturing, and freeform fabrication, can be generally classified into seven major technologies (Martinez-Garcia et al., 2021); material extrusion (Batchelder & Crump, 1999), material jetting (Gothait, 2001), binder jetting (Tochimoto & Kubo, 2004), vat photopolymerization (Hull, 1984), powder bed fusion (Deckard et al., 1992), direct energy deposition, and sheet object lamination (Feygin & Pak, 1999). Material extrusion and material jetting use nozzle and jetting head for extruding and jetting material, respectively. In the binder jet, the inkjet spreads the binder onto a powder to form the final object while vat photopolymerization applies a light foundation to the photosensitive resin. In the powder bed fusion technology, the top layer of powder is fused in the powder bed using a laser or electron beam followed by spreading the next layer. Finally, objects are made by joining sheets and cutting them to the desired form in the sheet object lamination variant of additive manufacturing.

The 3D printing procedure for extrusion-based production consists of the following steps. Assuming the ceramic powder fusing as the input material, light-curing resin and ball milling of methanol-based solvent are used to form a liquid slurry, which dries quickly after applying. Given 3D model requirements, i.e., dimensions, the semi-solid slurry will be then processed by a photomask projector to stabilize the material. In this procedure, the unilluminated parts of the object, which are semi-solid remains, act as a supporting structure for the final product. As a final step, the lamination procedure begins by laying several slurry layers on the forming plate to ensure that the finished parts do not stick to the molding board while being removed. A cooling system, i.e., the fan, is usually used to speed up the volatilization of the solvent in the slurry that is breached into the lower layers. The added layer gets thinner over time, and the powder becomes denser and more attached to the lower layer. Once the slurry is transitioned into a semi-solid state, the gas with volatile solvent should be discharged, followed by slow

evaporation of the solvent (Tsai et al., 2020).

Overall, additive manufacturing enhances production speed, quality, and flexibility, and reduces variable costs, i.e., logistics expenses (Demir et al., 2021; Haghdadati et al., 2021); however, further development is required to reduce fixed investment costs and improve know-how, which are the major barriers to its adoption (Yi et al., 2019). Given manufacturing time and cost as the critical factors, production scheduling is a much-needed tool to advance additive manufacturing towards end-part production. From a production scheduling standpoint, AMSP is different from the scheduling of subtractive manufacturing in that a single production run may involve several parts/geometries. That is, different geometries may constitute a generic job, which makes the jobs heterogeneous. In this definition, a build in the additive manufacturing procedure can be considered as a set of jobs in the conventional sense, which is identified by the geometry type and the number ( $n$ ) of parts to be produced for a particular production run, build.

AMSPs account for physical constraints (e.g., number and size of the 3D printers), dominant product features (e.g., main dimension, material), grouping in clusters and nesting in blocks (e.g., part orientation within the building volume), sequencing of customer orders (e.g., based on earliness and tardiness penalties), to optimize the overall performance (e.g., build time and cost) (Chergui et al., 2018; Fera et al., 2018; Kucukkoc, 2019). In the nesting procedure, parts should be grouped based on geometry, material, and due dates to maximize chamber volume utilization. Besides, arranging parts in the same build has a direct impact on the scheduling outcomes (Thompson et al., 2016). The existing scheduling literature either consider nesting of the parts (Aloui & Hadj-Hamou, 2021) or scheduling them (Kapadia et al., 2021) while studies considering simultaneous nesting and scheduling are relatively limited (Oh et al., 2020). In the most relevant problem from subtractive manufacturing literature, the scheduling of a single batch-processing machine with non-identical job sizes has been recently studied by (S. Zhou et al., 2021); their model does not account for build size restrictions and cannot handle the scheduling of parts under each builds. Our study addresses this limitation considering process constraints, product features, and customers deadlines in a 2D (dominant area), and M/M/S setting; Fig. 1 is an exemplary illustration of the addressed problem.

The following assumptions and notations are considered to model the M/M/S problem.

- The parts/geometries are grouped as a job (build).
- The exact volume of geometries is considered for calculation, which contains support structure and part removal space.

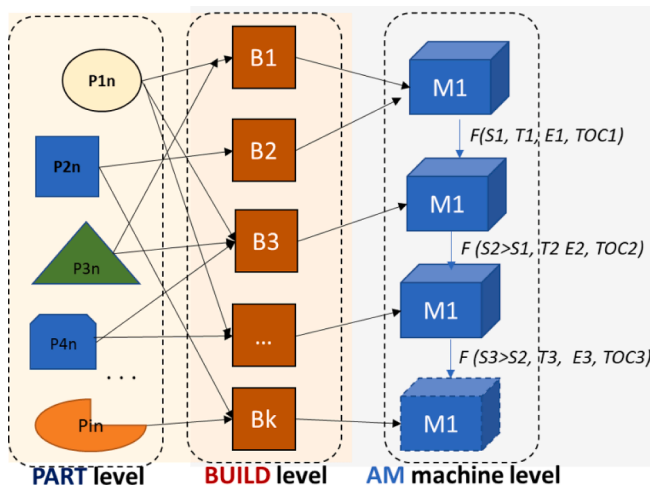


Fig. 1. Illustration of the M/M/S problem.

- Jobs are processed without interruptions, i.e., maintenance and downtime.
- Inventory costs for the injection material are assumed to be negligible.
- Considering a priori preference articulation, the objective weights are assumed to be known before production scheduling.

Given these assumptions and notations, the objective is to minimize the earliness-tardiness and operational costs, which are represented by  $F_S = \sum_{i=1}^{n_g} (\alpha E_i + \beta T_i) + \sum_{i=1}^{n_g} \gamma TOC_i$ . Finally, the following additive manufacturing-specific constraints were introduced by (Fera et al., 2018) to extend the production scheduling problems for the new application area.

$$\sum_{i=1}^{n_g} n_{ij} * V_i \leq V_{chamber}, \forall j \in \{1, \dots, n_b\} \quad (1)$$

$$\sum_{i=1}^{n_b} n_{ij} = d_i, \forall i \in \{1, \dots, n_g\} \quad (2)$$

$$\alpha, \beta, \gamma, TOC_i, V_i V_{chamber} \in R^+ \quad (3)$$

$$E_i, T_i, i, j, n_g, n_b \in Z^+ \quad (4)$$

Constraint set (1) ensures that the overall volume required by the parts/geometries does not exceed the chamber capacity. Eq. (2) indicate that the total number of geometries assigned to each build should be equal to the total demand for the respective part/geometry. Constraint sets (3) and (4) define the domains of variables and parameters. A metaheuristic algorithm is developed in the next section to optimize the AMSP with the above specifications.

### 3. Proposed algorithm

The basic Iterated Greedy algorithm is prone to early convergence in complex search spaces, and it often gets trapped in local optimality (Ying et al., 2020). Besides, the computational elements of the existing Iterated Greedy algorithms cannot effectively address the operational features of the AMSPs, which is different from that of the traditional production scheduling. This study develops a new benchmark algorithm, the AIG, which is customized for additive manufacturing features. For this purpose, the initialization and construction procedures are customized, and a local search procedure inspired by the Tabu concept is integrated into the search procedure to improve the exploitation power of the solution algorithm. The computational procedure of the AIG algorithm is presented in Fig. 2, followed by an elaboration on the major computational elements.

#### 3.1. Solution initialization

A three-step initialization procedure based on the 3D build concept is proposed to address the additive manufacturing requirements. For this purpose, the type-matrix in Table 1 is used as the input data to the initialization and encoding/decoding procedures. In this table, the rows and columns represent various print geometries ( $i$ ) and the number of builds required to print every geometry ( $j$ ), respectively. The geometries are different in shape, size, and support structure; hence, the columns with the same geometry can be swapped. The printing chamber for 3D printing, i.e., the build concept shown in Fig. 3, is the basis of defining this matrix. Considering a total of  $g$  geometries and  $b$  builds in the type-matrix, the initial solution is encoded as  $(n_{1,1}, \dots, n_{1,g} | n_{2,1}, \dots, n_{2,g} | \dots | n_{b,1}, \dots, n_{b,g})$ . The step-by-step guide to the solution initialization procedure is described below.

**Step 1.** Determine the number of columns and rows in the matrix. The number of columns is defined based on the number of geometries that should be printed. The total number of rows, which refers to the

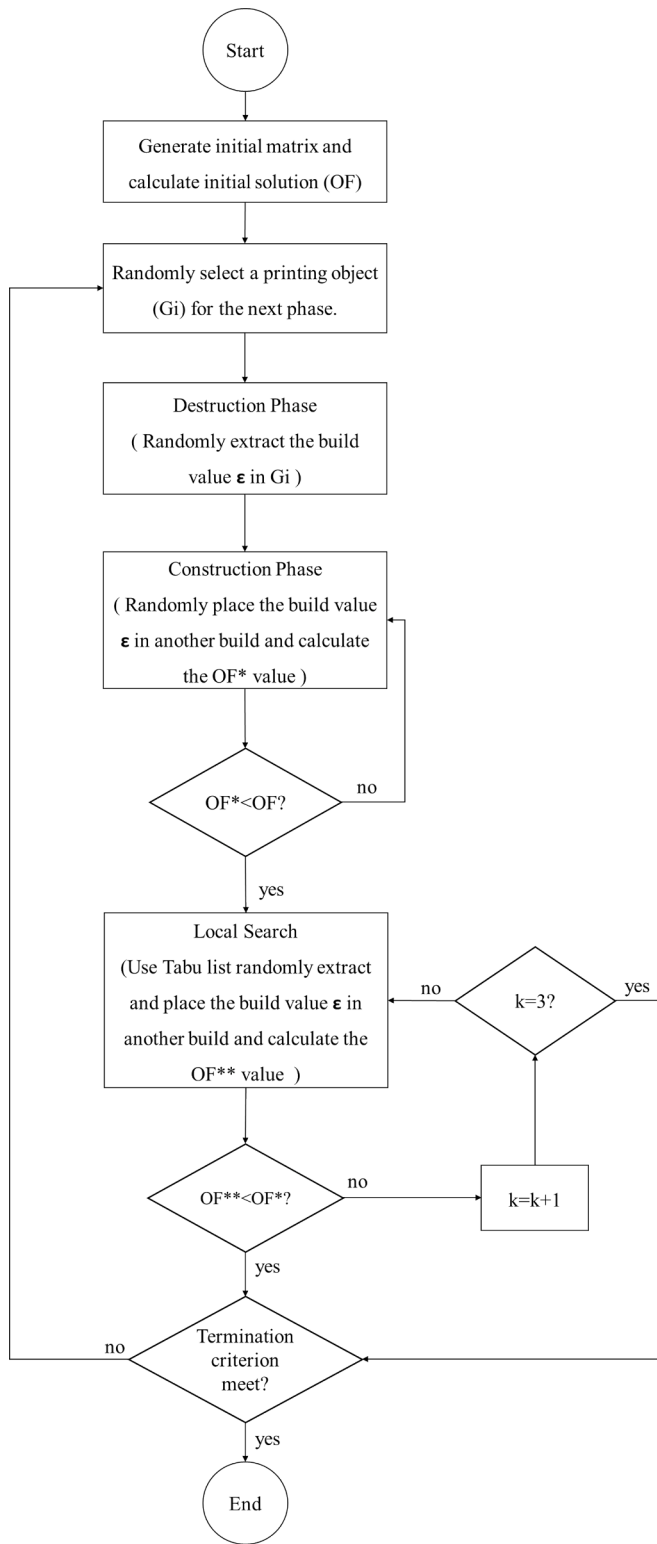


Fig. 2. The computational procedure of the Adjusted Iterated Greedy algorithm.

required build quantity, can be calculated using Equation (5). Considering that each build is only used by one machine, the same geometry volume,  $V_{chamber}$ , is applied. In this formulation, the volume of geometries is multiplied by the respective  $n_{ij}$  value from the matrix, which is then divided by the chamber volume.

Table 1  
Type matrix for solution initialization.

$n_{ij}$	Geometries (i)				$V_{chamber}$		
	1	2	...	$n_g$	$V_{used} (cm^3)$	$V_{available} (cm^3)$	
Build (j)	1	$n_{1,1}$	$n_{1,2}$	...	$n_{1,g}$	$V_1$	$V_{chamber} - V_1$
	2	$n_{2,1}$	$n_{2,2}$	...	$n_{2,g}$	$V_2$	$V_{chamber} - V_2$
	...	...	...	...	...	...	...
	$n_b$	$n_{b,1}$	$n_{ij}$	...	$n_{b,g}$	$V_b$	$V_{chamber} - V_b$

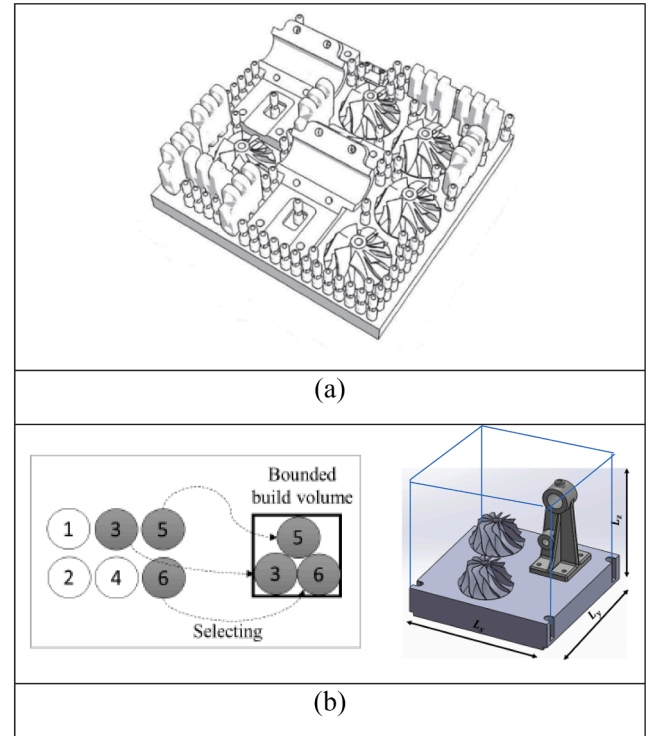


Fig. 3. Schematic representation of the exemplary (a) build structure, and (2) example of chamber constraint and geometry effect in Additive Manufacturing.

$$N_{build} = \frac{\sum_{j=1}^b \sum_{i=1}^g n_{ij} * V_i}{V_{chamber}} \quad (5)$$

**Step 2.** Given the initial matrix, select a random column and several random rows from the selected column. Insert a random geometry number into the selected build (row) and continue until all geometries (column) are inserted. Meanwhile, the procedure checks whether there is a violation of the volume constraint  $V_{available}$  during the insertion; if the constraint is violated, another build is randomly selected, and the quantity is inserted into it until the solution abides by the volume constraint.

**Step 3.** Calculate the fitness value of the complete solution.

### 3.2. Destruction mechanism

Given the initial solution in the first iteration and the current-best solution in other iterations, the destruction/construction procedure applies to restructure the solution to a better state. A new destruction method is developed to ensure the effectiveness of the search procedure. In this approach, geometries with a larger volume receive a higher priority for destruction because they significantly impact the volume constraint in the build procedure. Fig. 4(a) is used as an illustrative example to describe the four-step procedure explained below.

**Step 1.** Select the geometry with the largest volume, i.e., geometry 1

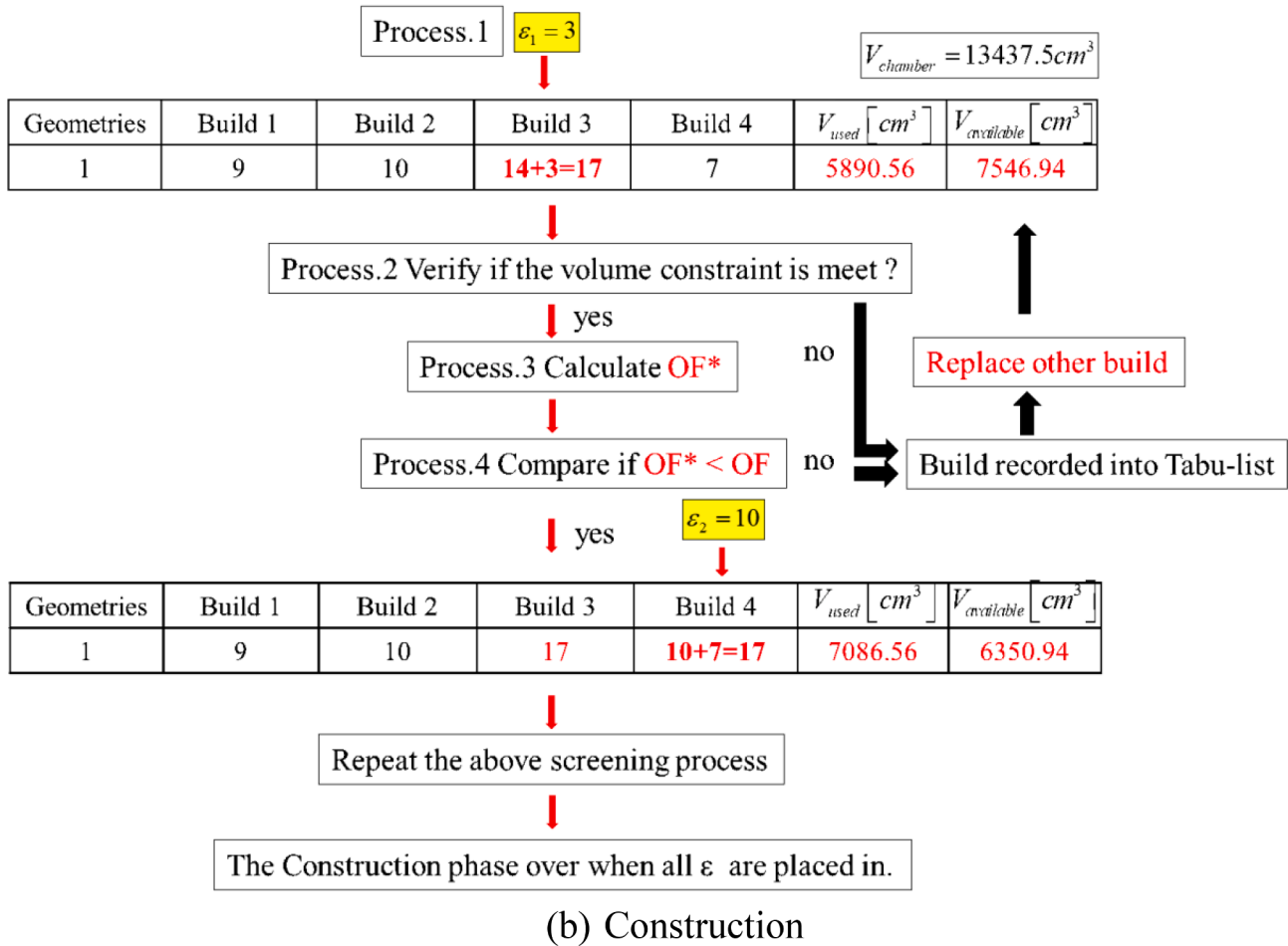
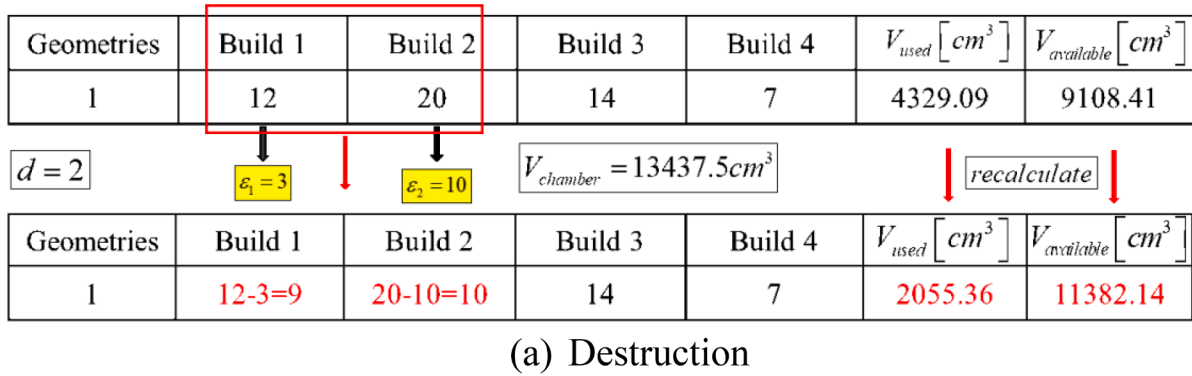


Fig. 4. Illustration of the (a) destruction and (b) construction procedures.

in column 1 of the illustrative example.

**Step 2.** Select  $d$  builds, randomly, with  $d$  being the destruction count. Assuming  $d = 2$  in the illustrative example, build 1 and build 2 are extracted in the destruction phase.

**Step 3.** Extract  $\epsilon \in [1, n_{ij}]$  geometries from the selected builds, i.e., 1 and 2 in the illustrative example. Assuming  $n_{1,1} = 12$ ,  $\epsilon$  will be a random integer between 1 and 12. In the illustrative example,  $\epsilon_1 = 3$  and  $\epsilon_2 = 10$ . The original number of builds should be deducted from  $\epsilon$  to obtain a new number after the destruction procedure.  $\epsilon_1$  and  $\epsilon_2$  values will be used as algorithm parameters in the construction phase.

**Step 4.** Update  $V_{available}$  of the new build for consideration in the construction phase.

### 3.3. Construction and local search mechanisms

Given the partial solution resulting from the destruction phase, as well as the updated  $\epsilon$  and  $V_{available}$  parameters, a three-step construction procedure is developed to generate new solutions. The procedure is explained in the following and illustrated using the example in Fig. 4(b).

**Step 1.** Add  $\epsilon$  values into the random builds (rows). Given  $\epsilon_1 = 3$  and  $\epsilon_2 = 10$  in the illustrative example and considering 3 and 4 positions of build 1 as the random locations, we have  $n_{1,3} + \epsilon_1, n_{1,4} + \epsilon_2$ .

**Step 2.** Check if the updated values violate the chamber volume constraint,  $V_{available}$ . In case of experiencing a violation, return to step 2 and select other random builds. This procedure continues until a feasible alternative is identified. The Tabu concept of the Tabu Search algorithm is adopted to record the builds that violate the constraint to improve the



procedure's efficiency. For example, if adding  $\varepsilon_1$  into build 3 violates the chamber volume constraint, it will not be considered a certain number of times; the same method applies for  $\varepsilon_2$ .

**Step 3.** Calculate the fitness value of the new solution. Proceed with the new build if it has resulted in a better fitness value, i.e.,  $f_{new} \leq f_{best}$ , otherwise, proceed to the next step considering the old solution.

**Step 4.** Solutions from the construction phase will be considered for a local search attempt. The Roulette Wheel Selection method is used to select a build; the larger the printing chamber is, the higher the chance to select the associated build. Next,  $\varepsilon$  is deducted from the selected build, keeping in mind that the volume constraint is not violated. The alternative solution will be accepted only if the resulting fitness function value is strictly better than that of the original solution.

### 3.4. Acceptance and stopping conditions

A new solution ( $\pi'$ ) is accepted if it is either associated with a strictly better fitness value than the current solution ( $\pi$ ) or the acceptance mechanism allows for accepting it despite having a less competitive fitness value. Discarding the solution with a worse fitness value may result in local optimality and early convergence. An acceptance mechanism inspired by the Simulated Annealing is adopted to alleviate this issue; (Hatami et al., 2015)'s mechanism showed to be more effective than others when it comes to escaping from local optimality. In this approach, the temperature value,  $T$ , and Relative Performance Deviation (RPD) of the new solution are the basis of regulating the acceptance condition; these values are calculated using Equations (6)-(7), where  $F(\pi)$  and  $F(\pi')$  represent the fitness value of the current and new solutions, respectively. Considering these formulations, the Acceptance Probability amounts to  $\alpha \leq e^{(-RPD/temperature)}$  with alpha being a random number between 0 and 1.

$$Temperature = T \times \frac{\sum_{i=1}^m \sum_{j=1}^n P_{ij}}{n \times m \times 10} \tag{6}$$

**Table 2**  
Case data parameters.

Instance	DD (day)	Q (parts)	V (cm <sup>3</sup> )	H (mm)	T <sub>prep</sub> (hours)	Penalty (% daily)	S <sub>max</sub> (cm <sup>3</sup> )
1	120	7	146	50.55	1	1	82.1
2	60	5	52.87	85	1	2	120
3	180	10	108.9	62.5	1	2	344.22
4	120	7	64.17	37.73	1	1.5	21
5	120	5	200.8	183.4	0.5	3	208.08
6	90	5	66.94	56.02	1	1.5	178.72
7	120	5	90.15	95	0.5	2	57.04
8	120	8	188.2	162.5	1	2	104.56
9	150	9	33.65	32.29	1	1.5	97.12
10	180	9	290.2	186.6	1	1.5	112.28
11	60	5	62	150	0.5	1	176.71
12	180	10	6	73	1	2	41.85
13	180	10	9	65	0.4	1	33.18
14	90	8	56	115	0.6	2	103.869
15	120	5	17	100	0.4	1	213.82
16	150	8	44	165	0.4	3	78.54
17	120	7	4.87	100	0.1	1	3.14
18	60	5	2.9	22	0.2	1	38.48
19	180	10	112	70	0.4	1	116.9
20	90	5	150	122	0.4	2	201.06
21	150	8	375	160	0.7	1	4.91
22	60	5	17.5	25	0.1	1	28.27
23	90	6	36	60	0.2	1	12.57
24	120	7	13.4	40	0.2	1	10.18
25	90	5	22.6	36	0.3	2	9.62
26	120	7	7	35	0.4	2	12.57
27	60	4	11	40	0.4	1	10.18
28	90	5	4	45	0.4	2	9.62
29	120	7	15	50	0.4	2	19.63
30	180	10	0.569	20	0.4	2	3.14

$$RPD = \frac{F(\pi') - F(\pi)}{F(\pi)} \times 100 \tag{7}$$

Finally, the metaheuristics are all compiled and tested considering the same stopping criterion to ensure a fair comparison between the benchmark algorithms. For this purpose, Maximum CPU time is considered as the stopping condition.

## 4. Results analysis

This section elaborates on the numerical experiments conducted to evaluate the effectiveness of the AIG algorithm. The ITS algorithm developed by (Fera et al., 2020), which is the best available approach for solving the AMSPs, is considered as the baseline algorithm. All the benchmark algorithms are coded and compiled on a personal computer with the following specs: Intel® Core™ i7-3770 CPU 3.40 GHz processor, 32 Gb of RAM, and Windows 10 64-bit Operating System.

Small-, medium-, and large-scale instances are considered to conduct the numerical experiments. The problem specifications shown in Table 2 are considered for the generation of random instances. In this table,  $PN$  (print number),  $DD$  (due date),  $Q$  (quantity),  $V$  (volume),  $H$  (height),  $T_{prep}$  (preparation time) define the specifications of the print objects. Besides,  $Penalty$  and  $S_{max}$  represent the lateness price and the maximum area of each print object. The small-scale instance set by (Fera et al., 2020) is extended to make a total of 20 configurations, i.e., S01- S20. The medium- (M01-M20) and large-size instances (L01-L20) are generated randomly considering the same object features, each in 20 distinct workloads. A build chamber of size 13437.5 cm<sup>3</sup> is considered for all the test instances. Finally, the earliness, tardiness, and total cost weights in this paper are set to  $\alpha = 0.4$ ,  $\beta = 0.4$ , and  $\gamma = 0.2$ , respectively.

To begin with the experiments, the extracted geometric number ( $\varepsilon$ ) is generated randomly from interval  $[1, n_{ij}]$ . Given the destruction value fixed at  $d = 2$ , calibration test is conducted to determine the maximum CPU time (i.e., the stopping criterion). For this purpose, convergence under various problem sizes (i.e., workloads) is considered. We found

that the benchmark algorithms require 10, 30, and 50 ms of the maximum CPU time to find a (near-) optimum solution to the small-, medium-, and large-scale instances, respectively. Next, the minimum (*Min*), average (*Ave*), and standard deviation (*StD*) are considered to analyze the performance of the algorithm for solving the test instances. The former measure refers to the best solution obtained by every algorithm, and the latter two measures determine the stability of the algorithms' performance. Results for small-, medium-, and large-size instances are provided in Tables 3-5, respectively.

Considering the small-size instances in Table 3, the AIG algorithm yields the BFS in 15 out of 20 cases, and the ITS algorithm finds better solutions to S02, S04, S06, S11, and S13 instances. Besides, AIG shows to be more stable in 18 out of 20 small-size instances. From the medium-size instances M01-M20 in Table 4, the AIG performs better than the ITS algorithm in 14 cases while the remainder of the BFS, i.e., for M02, M05, M07, M09, M19, and M20 instances, are yielded by the ITS. According to Table 5, the AIG algorithm outperforms in all large-scale test instances considering both solution quality and the stability of the metaheuristic, showing that it is a more reliable optimization algorithm for industry-scale applications.

As the next step to analyzing the results, the extent of improvement in the solution quality is analyzed with respect to the RPD, calculated using Equation (8). A smaller RPD value is desired, and larger RPD values specify a larger deviation from the BFS for every instance. Besides, Average Relative Performance Deviation (ARPD) is used to show the overall extent of difference between the performance of the algorithms in terms of solution quality.

$$RPD = \frac{Fitness - Fitness^{best}}{Fitness^{best}} \times 100 \tag{8}$$

Table 6 provides the RPD and ARPD values. The first important observation is that the average RPD recorded by AIG in small-, medium-, and large-size instances are considerably better than those of ITS. In the small- and medium-size instances, however, the average value of AIG is slightly better than that of ITS. However, and considering the large-size instances, the average RPD of the AIG algorithm (which amounts to 0.0461) is meaningfully smaller than ITS with the RPD value of 0.1716. Except for S04 and M20 where the ITS algorithm yielded better solutions, the rest of the benchmarks are dominated by the AIG algorithm.

A statistical test of significance is finally conducted to determine whether the resulting improvement in each problem category is significant. For this purpose, the null hypothesis indicates that there is no significant difference between the performance of the benchmarked

**Table 3**  
Experimental results considering small-size instances (best in bold).

Instances	ITS			AIG		
	Min	Ave	StD	Min	Ave	StD
S01	824	838	11	<b>810</b>	<b>822</b>	<b>8</b>
S02	<b>810</b>	830	9	817	<b>828</b>	<b>5</b>
S03	824	838	<b>7</b>	<b>810</b>	<b>827</b>	<b>8</b>
S04	<b>810</b>	<b>829</b>	16	825	835	<b>6</b>
S05	827	836	<b>7</b>	<b>812</b>	<b>822</b>	<b>5</b>
S06	<b>810</b>	830	12	812	<b>827</b>	<b>7</b>
S07	824	849	16	<b>813</b>	<b>827</b>	<b>8</b>
S08	810	826	9	<b>805</b>	<b>820</b>	<b>8</b>
S09	809	832	12	<b>804</b>	<b>820</b>	<b>10</b>
S10	811	832	11	<b>809</b>	<b>816</b>	<b>7</b>
S11	<b>804</b>	840	19	815	<b>834</b>	<b>9</b>
S12	818	839	23	<b>809</b>	<b>827</b>	<b>10</b>
S13	<b>807</b>	838	18	808	<b>816</b>	<b>6</b>
S14	825	870	16	<b>812</b>	<b>830</b>	<b>7</b>
S15	<b>836</b>	849	6	820	<b>826</b>	<b>5</b>
S16	818	836	12	<b>813</b>	<b>834</b>	<b>7</b>
S17	814	834	<b>12</b>	<b>808</b>	<b>820</b>	<b>13</b>
S18	812	839	14	<b>809</b>	<b>830</b>	<b>8</b>
S19	811	830	10	<b>805</b>	<b>815</b>	<b>6</b>
S20	834	850	8	<b>815</b>	<b>826</b>	<b>6</b>

**Table 4**  
Experimental results considering medium-size instances (best in bold).

Instances	ITS			AIG		
	Min	Ave	StD	Min	Ave	StD
M01	1328	1333	<b>4</b>	<b>1319</b>	<b>1329</b>	<b>5</b>
M02	<b>1308</b>	1335	12	1326	<b>1331</b>	<b>4</b>
M03	1289	1314	<b>7</b>	<b>1283</b>	<b>1312</b>	<b>10</b>
M04	1303	1313	<b>4</b>	<b>1302</b>	<b>1307</b>	<b>3</b>
M05	<b>1292</b>	1321	14	1311	<b>1319</b>	<b>5</b>
M06	1307	1316	5	<b>1306</b>	<b>1315</b>	<b>4</b>
M07	<b>1317</b>	<b>1329</b>	5	1326	1330	<b>3</b>
M08	1324	1332	<b>4</b>	<b>1322</b>	<b>1325</b>	<b>2</b>
M09	<b>1284</b>	<b>1303</b>	6	1291	<b>1303</b>	<b>4</b>
M10	1356	1368	<b>6</b>	<b>1333</b>	<b>1351</b>	<b>11</b>
M11	1306	<b>1325</b>	<b>12</b>	<b>1302</b>	<b>1325</b>	<b>13</b>
M12	1332	1341	5	<b>1324</b>	<b>1338</b>	<b>5</b>
M13	1290	<b>1305</b>	12	<b>1288</b>	1310	<b>8</b>
M14	1338	1344	<b>4</b>	<b>1329</b>	<b>1341</b>	<b>6</b>
M15	1317	1323	5	<b>1306</b>	<b>1313</b>	<b>4</b>
M16	1336	1341	<b>4</b>	<b>1318</b>	<b>1334</b>	<b>8</b>
M17	1309	1316	<b>4</b>	<b>1308</b>	<b>1314</b>	<b>3</b>
M18	1295	1307	<b>9</b>	<b>1283</b>	<b>1303</b>	<b>12</b>
M19	<b>1301</b>	1321	9	1306	<b>1315</b>	<b>7</b>
M20	<b>1277</b>	<b>1299</b>	<b>9</b>	1294	1308	<b>9</b>

**Table 5**  
Experimental results considering large-size instances (best in bold).

Instances	ITS			AIG		
	Min	Ave	StD	Min	Ave	StD
L01	1581	1650	38	<b>1369</b>	<b>1429</b>	<b>28</b>
L02	1463	1564	65	<b>1374</b>	<b>1450</b>	<b>34</b>
L03	1566	1670	52	<b>1397</b>	<b>1464</b>	<b>40</b>
L04	1407	1658	73	<b>1373</b>	<b>1445</b>	<b>34</b>
L05	1575	1667	51	<b>1383</b>	<b>1430</b>	<b>39</b>
L06	1530	1633	49	<b>1407</b>	<b>1473</b>	<b>48</b>
L07	1540	1637	60	<b>1417</b>	<b>1454</b>	<b>27</b>
L08	1521	1618	41	<b>1419</b>	<b>1485</b>	<b>33</b>
L09	1552	1638	54	<b>1428</b>	<b>1474</b>	<b>32</b>
L10	1554	1671	58	<b>1375</b>	<b>1427</b>	<b>42</b>
L11	1472	1543	47	<b>1366</b>	<b>1435</b>	<b>42</b>
L12	1527	1595	49	<b>1376</b>	<b>1428</b>	<b>33</b>
L13	1536	1644	44	<b>1380</b>	<b>1441</b>	<b>31</b>
L14	1540	1617	51	<b>1378</b>	<b>1437</b>	<b>30</b>
L15	1517	1648	62	<b>1344</b>	<b>1453</b>	<b>56</b>
L16	1517	1581	35	<b>1367</b>	<b>1436</b>	<b>31</b>
L17	1521	1628	47	<b>1360</b>	<b>1423</b>	<b>32</b>
L18	1586	1662	<b>40</b>	<b>1440</b>	<b>1528</b>	<b>44</b>
L19	1482	1602	65	<b>1396</b>	<b>1470</b>	<b>33</b>
L20	1461	1544	54	<b>1370</b>	<b>1414</b>	<b>29</b>

algorithms. The *t*-test results and the respective *p*-values are provided in Table 7, where there is enough evidence to refute the null hypothesis. That is, we can claim with 95 percent confidence that the developed AIG algorithm in our study is superior to the ITS algorithm. AIG can be now considered as a strong benchmark algorithm for future developments of the AMSP and its extensions.

**5. Conclusions**

Additive manufacturing consists of depositing raw material, layer by layer, to produce parts/products based on digital design documents. In contrast with traditional production techniques, which are based on material removal and/or injection molding, additive manufacturing can more effectively deal with complex geometries and use compound material in the production process. It also has implications for simplifying supply chain operations. Overall, additive manufacturing is expected to replace the traditional production processes in certain industries. To contribute to the emerging literature of additive manufacturing, this study developed an effective solution algorithm for optimizing the

**Table 6**  
Relative performance deviation across test instances (best in bold).

Instance	ITS	AIG	Instance	ITS	AIG	Instance	ITS	AIG
S01	0.0350	<b>0.0155</b>	M01	0.011	<b>0.0081</b>	L01	0.2055	<b>0.0439</b>
S02	0.0248	<b>0.0222</b>	M02	0.021	<b>0.0182</b>	L02	0.1385	<b>0.0557</b>
S03	0.0339	<b>0.0205</b>	M03	0.024	<b>0.0228</b>	L03	0.1949	<b>0.0477</b>
S04	<b>0.0243</b>	0.0317	M04	0.008	<b>0.0042</b>	L04	0.2077	<b>0.0523</b>
S05	0.0299	<b>0.0125</b>	M05	0.022	<b>0.0209</b>	L05	0.2050	<b>0.0338</b>
S06	0.0256	<b>0.0216</b>	M06	0.008	<b>0.0076</b>	L06	0.1606	<b>0.0473</b>
S07	0.0440	<b>0.0178</b>	M07	<b>0.009</b>	0.0095	L07	0.1552	<b>0.0261</b>
S08	0.0262	<b>0.0184</b>	M08	0.007	<b>0.0025</b>	L08	0.1409	<b>0.0465</b>
S09	0.0360	<b>0.0203</b>	M09	0.015	<b>0.0148</b>	L09	0.1468	<b>0.0322</b>
S10	0.0290	<b>0.0081</b>	M10	0.027	<b>0.0135</b>	L10	0.2152	<b>0.0380</b>
S11	0.0456	<b>0.0379</b>	M11	<b>0.018</b>	0.0181	L11	0.1300	<b>0.0509</b>
S12	0.0372	<b>0.0214</b>	M12	0.013	<b>0.0101</b>	L12	0.1589	<b>0.0374</b>
S13	0.0387	<b>0.0114</b>	M13	0.013	<b>0.0172</b>	L13	0.1909	<b>0.0437</b>
S14	0.0722	<b>0.0221</b>	M14	0.011	<b>0.0089</b>	L14	0.1735	<b>0.0429</b>
S15	0.0355	<b>0.0077</b>	M15	0.014	<b>0.0060</b>	L15	0.2261	<b>0.0809</b>
S16	0.0288	<b>0.0257</b>	M16	0.018	<b>0.0120</b>	L16	0.1567	<b>0.0504</b>
S17	0.0321	<b>0.0140</b>	M17	0.006	<b>0.0050</b>	L17	0.1970	<b>0.0459</b>
S18	0.0374	<b>0.0265</b>	M18	0.019	<b>0.0157</b>	L18	0.1538	<b>0.0605</b>
S19	0.0312	<b>0.0127</b>	M19	0.015	<b>0.0110</b>	L19	0.1474	<b>0.0531</b>
S20	0.0426	<b>0.0137</b>	M20	<b>0.017</b>	0.0248	L20	0.1267	<b>0.0317</b>
ARPD	0.0355	<b>0.0191</b>	-	0.0148	<b>0.0125</b>	-	0.1716	<b>0.0461</b>

**Table 7**  
Statistical test of significance comparing AIG and ITS.

Instance	Difference			T	Critical <i>t</i>	DoF	<i>P</i> -value
	Ave	StD	S.E.				
S01-S20	0.0163	0.0125	0.0028	5.895	2.0930	19	0.000
M01-M20	0.0022	0.0042	0.0009	2.355	2.0930	19	0.029
L01-L20	0.1255	0.0304	0.1113	18.491	2.0930	19	0.000

StD: Standard Deviation, S.E.: Standard Error, DoF: Degree of Freedom.

AMSPs; the objective was to minimize the printing time/cost by grouping parts into batches (jobs) and determining the print permutation of the batches considering the utilization of the build chamber of the printing machine. New search mechanisms were developed to effectively address the additive manufacturing features. An extended testbed was used to conduct the numerical experiments. Results confirm the AIG algorithm's superiority in terms of solution quality and stability with an average relative performance difference of 0.0259 compared to that of the best-existing solution algorithm with 0.0739.

This study can be considered as a baseline for further developments of the scheduling problems and algorithms in additive manufacturing. The first suggestion for future research comes from considering case-specific technical features of additive manufacturing for developing new constraints. For example, the print object shape can be considered while accounting for a mixed setting. Besides, classic scheduling features like setup times and time constraints should be added to the AMSPs to facilitate its real-world applications. As a second direction, one can combine the scheduling problems of material extrusion, removal, and assembly for situations where the parts built through additive and traditional production processes should be assembled to form the final product. As a third promising research direction, one can develop distributed scheduling problems for simultaneously scheduling subtractive or injection molding and additive manufacturing-based operations. Next, our benchmark algorithm can be used as a baseline to develop more effective and efficient solution algorithms for solving the AMSP and its extensions. For example, discrete Jaya, the multi-temperature simulated annealing, chaos-enhanced simulated annealing, and mixed-variable differential evolution algorithm, among other state-of-the-art algorithms can be adjusted to work in compliance with additive manufacturing scheduling requirements. Finally, our study considers a priori performance articulation scheme for the optimization of the multi-objective problem. Future works should develop multi-

objective solution algorithms to provide a set of optimum solutions for possible trade-offs to address AMSPs with conflicting objectives and interfering jobs.

#### CRediT authorship contribution statement

**Kuo-Ching Ying:** Conceptualization, Methodology, Validation, Software, Resources, Project administration, Funding acquisition. **Fabio Fruggiero:** Conceptualization, Validation, Visualization. **Pourya Pourhejazy:** Writing – original draft, Writing – review & editing, Investigation. **Bo-Yun Lee:** Methodology, Formal analysis, Data curation.

#### Declaration of Competing Interest

The authors declare that they have no known competing financial interests or personal relationships that could have appeared to influence the work reported in this paper.

#### References

- Aloui, A., & Hadj-Hamou, K. (2021). A heuristic approach for a scheduling problem in additive manufacturing under technological constraints. *Computers & Industrial Engineering*, 154, 107115. <https://doi.org/10.1016/j.cie.2021.107115>
- Ank, O. A. (2021). Additive manufacturing scheduling problem considering assembly operations of parts. *Operational Research*. <https://doi.org/10.1007/s12351-021-00649-y>
- Batchelder, J. S., & Crump, S. S. (1999). Method for rapid prototyping of solid models. *Google Patents*.
- Bikas, H., Stavropoulos, P., & Chryssolouris, G. (2016). Additive manufacturing methods and modelling approaches: A critical review. *The International Journal of Advanced Manufacturing Technology*, 83(1–4), 389–405. <https://doi.org/10.1007/s00170-015-7576-2>
- Blakey-Milner, B., Gradl, P., Snedden, G., Brooks, M., Pitot, J., Lopez, E., ... du Plessis, A. (2021). Metal additive manufacturing in aerospace: A review. *Materials & Design*, 209, 110008. <https://doi.org/10.1016/j.matdes.2021.110008>
- Chergui, A., Hadj-Hamou, K., & Vignat, F. (2018). Production scheduling and nesting in additive manufacturing. *Computers & Industrial Engineering*, 126, 292–301. <https://doi.org/10.1016/j.cie.2018.09.048>
- Cruz Sanchez, F. A., Boudaoud, H., Camargo, M., & Pearce, J. M. (2020). Plastic recycling in additive manufacturing: A systematic literature review and opportunities for the circular economy. *Journal of Cleaner Production*, 264, 121602. <https://doi.org/10.1016/j.jclepro.2020.121602>
- Deckard, C. R., Beaman, J. J., & Darrah, J. F. (1992). Method for selective laser sintering with layerwise cross-scanning. *Google Patents*.
- Demir, E., Eysers, D., & Huang, Y. (2021). Competing through the last mile: Strategic 3D printing in a city logistics context. *Computers & Operations Research*, 131, 105248. <https://doi.org/10.1016/j.cor.2021.105248>



- Reddy, R. D. P., & Sharma, V. (2020). Additive manufacturing in drug delivery applications: A review. *International Journal of Pharmaceutics*, 589, 119820. <https://doi.org/10.1016/j.ijpharm.2020.119820>
- Fera, M., Fruggiero, F., Lambiase, A., Macchiaroli, R., & Todisco, V. (2018). A modified genetic algorithm for time and cost optimization of an additive manufacturing single-machine scheduling. *International Journal of Industrial Engineering Computations*, 423–438. <https://doi.org/10.5267/j.ijiec.2018.1.001>
- Fera, M., Macchiaroli, R., Fruggiero, F., & Lambiase, A. (2020). A modified tabu search algorithm for the single-machine scheduling problem using additive manufacturing technology. *International Journal of Industrial Engineering Computations*, 401–414. <https://doi.org/10.5267/j.ijiec.2020.1.001>
- Feygin, M., & Pak, S. S. (1999). Laminated object manufacturing apparatus and method. *Google Patents*.
- Gisario, A., Kazarian, M., Martina, F., & Mehrpouya, M. (2019). Metal additive manufacturing in the commercial aviation industry: A review. *Journal of Manufacturing Systems*, 53, 124–149. <https://doi.org/10.1016/j.jmsy.2019.08.005>
- Gothait, H. (2001). *Apparatus and method for three dimensional model printing*. Google Patents.
- Haghdadi, N., Laleh, M., Moyle, M., & Primig, S. (2021). Additive manufacturing of steels: A review of achievements and challenges. *Journal of Materials Science*, 56(1), 64–107. <https://doi.org/10.1007/s10853-020-05109-0>
- Hatami, S., Ruiz, R., & Andrés-Romano, C. (2015). Heuristics and metaheuristics for the distributed assembly permutation flowshop scheduling problem with sequence dependent setup times. *International Journal of Production Economics*, 169, 76–88. <https://doi.org/10.1016/j.ijpe.2015.07.027>
- Hull, C. W. (1984). Apparatus for production of three-dimensional objects by stereolithography. *United States Patent, Appl., No. 638905*, Filed.
- Kapadia, M. S., Uzsoy, R., Starly, B., & Warsing, D. P. (2021). A genetic algorithm for order acceptance and scheduling in additive manufacturing. *International Journal of Production Research*, 1–18. <https://doi.org/10.1080/00207543.2021.1991023>
- Khorram Niaki, M., & Nonino, F. (2017). Additive manufacturing management: A review and future research agenda. *International Journal of Production Research*, 55(5), 1419–1439. <https://doi.org/10.1080/00207543.2016.1229064>
- Kucukkoc, I. (2019). MILP models to minimise makespan in additive manufacturing machine scheduling problems. *Computers & Operations Research*, 105, 58–67. <https://doi.org/10.1016/j.cor.2019.01.006>
- Li, Q., Kucukkoc, I., & Zhang, D. Z. (2017). Production planning in additive manufacturing and 3D printing. *Computers & Operations Research*, 83, 157–172. <https://doi.org/10.1016/j.cor.2017.01.013>
- Luzon, Y., & Khmelitsky, E. (2019). Job sizing and sequencing in additive manufacturing to control process deterioration. *IIE Transactions*, 51(2), 181–191. <https://doi.org/10.1080/24725854.2018.1460518>
- Martínez-García, A., Monzón, M., & Paz, R. (2021). Standards for additive manufacturing technologies: Structure and impact. In *Additive Manufacturing* (pp. 395–408). Elsevier.
- Naghshineh, B., Ribeiro, A., Jacinto, C., & Carvalho, H. (2021). Social impacts of additive manufacturing: A stakeholder-driven framework. *Technological Forecasting and Social Change*, 164, 120368. <https://doi.org/10.1016/j.techfore.2020.120368>
- Oh, Y., Witherell, P., Lu, Y., & Sprock, T. (2020). Nesting and scheduling problems for additive manufacturing: A taxonomy and review. *Additive Manufacturing*, 36, 101492. <https://doi.org/10.1016/j.addma.2020.101492>
- Oh, Y., Zhou, C., & Behdad, S. (2018). Part decomposition and 2D batch placement in single-machine additive manufacturing systems. *Journal of Manufacturing Systems*, 48, 131–139. <https://doi.org/10.1016/j.jmsy.2018.07.006>
- Paolini, A., Kollmannsberger, S., & Rank, E. (2019). Additive manufacturing in construction: A review on processes, applications, and digital planning methods. *Additive Manufacturing*, 30, 100894. <https://doi.org/10.1016/j.addma.2019.100894>
- Pérez, M., Carou, D., Rubio, E. M., & Teti, R. (2020). Current advances in additive manufacturing. *Procedia CIRP*, 88, 439–444. <https://doi.org/10.1016/j.procir.2020.05.076>
- Ransikarbun, K., Ha, S., Ma, J., & Kim, N. (2017). Multi-objective optimization analysis for part-to-Printer assignment in a network of 3D fused deposition modeling. *Journal of Manufacturing Systems*, 43, 35–46. <https://doi.org/10.1016/j.jmsy.2017.02.012>
- Rudolph, J.-P., & Emmelmann, C. (2017). A Cloud-based Platform for Automated Order Processing in Additive Manufacturing. *Procedia CIRP*, 63, 412–417. <https://doi.org/10.1016/j.procir.2017.03.087>
- Salmi, M., Ituarte, I. F., Chekurov, S., & Huotilainen, E. (2016). Effect of build orientation in 3D printing production for material extrusion, material jetting, binder jetting, sheet object lamination, vat photopolymerisation, and powder bed fusion. *International Journal of Collaborative Enterprise*, 5(3/4), 218. <https://doi.org/10.1504/IJCENT.2016.082334>
- Sepasgozar, S. M. E., Shi, A., Yang, L., Shirowzhan, S., & Edwards, D. J. (2020). Additive manufacturing applications for industry 4.0: A systematic critical review. *Buildings*, 10(12), 231. <https://doi.org/10.3390/buildings10120231>
- Sonar, H. C., Khanzode, V., & Akarte, M. (2020). A conceptual framework on implementing additive manufacturing technology towards firm competitiveness. *International Journal of Global Business and Competitiveness*, 15(2), 121–135. <https://doi.org/10.1007/s42943-020-00015-3>
- Song, Y., Li, Y., Song, W., Yee, K., Lee, K.-Y., & Tagarielli, V. L. (2017). Measurements of the mechanical response of unidirectional 3D-printed PLA. *Materials & Design*, 123, 154–164. <https://doi.org/10.1016/j.matdes.2017.03.051>
- Sun, C., Wang, Y., McMurtrey, M. D., Jerred, N. D., Liou, F., & Li, J. (2021). Additive manufacturing for energy: A review. *Applied Energy*, 282, 116041. <https://doi.org/10.1016/j.apenergy.2020.116041>
- Thompson, M. K., Moroni, G., Vaneker, T., Fadel, G., Campbell, R. I., Gibson, I., ... Martina, F. (2016). Design for Additive Manufacturing: Trends, opportunities, considerations, and constraints. *CIRP Annals*, 65(2), 737–760. <https://doi.org/10.1016/j.cirp.2016.05.004>
- Tochimoto, S., & Kubo, N. (2004). *Apparatus for forming a three-dimensional product*. Google Patents.
- Tönissen, D. D., & Schlicher, L. (2021). Using 3D-printing in disaster response: The two-stage stochastic 3D-printing knapsack problem. *Computers & Operations Research*, 133, 105356. <https://doi.org/10.1016/j.cor.2021.105356>
- Tsai, T.-H., Jeyaprasath, N., & Yang, C.-H. (2020). Non-destructive evaluations of 3D printed ceramic teeth: Young's modulus and defect detections. *Ceramics International*, 46(14), 22987–22998.
- Vernon, T., & Peckham, D. (2002). The benefits of 3D modelling and animation in medical teaching. *Journal of Audiovisual Media in Medicine*, 25(4), 142–148. <https://doi.org/10.1080/0140511021000051117>
- Yi, L., Gläßner, C., & Aurich, J. C. (2019). How to integrate additive manufacturing technologies into manufacturing systems successfully: A perspective from the commercial vehicle industry. *Journal of Manufacturing Systems*, 53, 195–211. <https://doi.org/10.1016/j.jmsy.2019.09.007>
- Ying, K.-C., Pourhejazy, P., Cheng, C.-Y., & Syu, R.-S. (2020). Supply chain-oriented permutation flowshop scheduling considering flexible assembly and setup times. *International Journal of Production Research*, 58(20), 1–24. <https://doi.org/10.1080/00207543.2020.1842938>
- Zhang, Y., Bernard, A., Harik, R., & Fadel, G. (2018). A new method for single-layer-part nesting in additive manufacturing. *Rapid Prototyping Journal*, 24(5), 840–854. <https://doi.org/10.1108/RPJ-01-2017-0008>
- Zhou, L., Zhang, L., Laili, Y., Zhao, C., & Xiao, Y. (2018). Multi-task scheduling of distributed 3D printing services in cloud manufacturing. *The International Journal of Advanced Manufacturing Technology*, 96(9–12), 3003–3017. <https://doi.org/10.1007/s00170-017-1543-z>
- Zhou, S., Xing, L., Zheng, X., Du, N., Wang, L., & Zhang, Q. (2021). A Self-Adaptive Differential Evolution Algorithm for Scheduling a Single Batch-Processing Machine With Arbitrary Job Sizes and Release Times. *IEEE Transactions on Cybernetics*, 51(3), 1430–1442. <https://doi.org/10.1109/TCYB.2019.2939219>